# Energy Efficiency Optimization in SWIPT Enabled WSNs for Smart Agriculture

Weidang Lu, *Senior Member, IEEE*, Xiaohan Xu, Guoxing Huang, Bo Li, *Member, IEEE*, Yuan Wu, *Senior Member, IEEE*, Nan Zhao, *Senior Member, IEEE*, and F. Richard Yu, *Fellow, IEEE*

***Abstract*—Smart agriculture is able to optimize the information resources of agriculture, which can improve the quality and productivity of agricultural products. Wireless sensor networks (WSNs) provide smart agriculture with effective solutions for collecting, transmitting, and processing of information. However, the large number of sensor networks consume too much energy that violates the principle of green communication. Simultaneous wireless information and power transfer (SWIPT) technology utilizes radio-frequency signals to transmit information and provide energy to WSNs, which can extend the lifetime of WSNs effectively. In this article, an architecture design of smart agriculture is first proposed by exploiting the SWIPT. Then, an energy efficiency optimization scheme is studied to achieve green communication, in which the subcarriers' pairing and power allocation are jointly optimized. The process of communication is divided into two phases. Specifically, in the first phase, source sensor sends information to relay sensor and destination sensor. Relay sensor utilizes a part of the subcarriers to receive the information, and utilizes the remaining subcarriers to collect energy. Destination sensor uses all the subcarriers to receive the information. In the second phase, relay sensor utilizes the energy collected in the first phase to forward the information to destination sensor. An effective iterative optimization algorithm is proposed to resolve the proposed optimization problem through Lagrangian dual function. Simulation results validate that the performance of the algorithm can improve energy efficiency of the system effectively.**

***Index Terms*—Power allocation, simultaneous wireless information and power transfer (SWIPT), subcarrier allocation, smart agriculture, wireless sensor networks (WSNs).**

## I. Introduction

THE POPULATION of the world is expected to be 9–10 billion, and the demand of food will increase to 60–70% by 2050. Meanwhile, it is requested minimal negative impacts on the environment, such as reducing the emissions of greenhouse gas and the consumption of water, which poses a critical challenge to the existing agriculture [1]. With the rising of the Internet of Things (IoT) technology [2], [3], it has provided strong technical support for agricultural development and accelerated the speed of agricultural transformation [4].

Through the deployment of wireless sensor networks (WSNs), smart agriculture is able to collect various information on the farm [5]–[8], e.g., the temperature and humidity of the greenhouse, the PH of the soil, and the concentration of CO2, as shown in Fig. 1, which can increase the agricultural production with real-time information monitoring [9], [10]. To realize smart agriculture, a massive number of sensor nodes need to be deployed. However, these sensor nodes are size constrained with low-capacity battery. Once the battery is exhausted, the sensor nodes will fail to work, which reduces the lifetime of the system. Therefore, it is important to design an efficient power supply mechanism for these low-powered sensor nodes.

Energy harvesting (EH) is a valid method to provide energy supply through harvesting energy from environmental resources [11], [12], e.g., solar, thermoelectricity, and wind. In [13], the sensor nodes are powered by harvesting energy from solar, which can effectively extend the lifetime of WSNs. [14] proposed an optimized wind EH system to sustain the operation of sensor nodes. However, these ambient energy source are unstable, which cannot provide sustainable energy supply. Moreover, in smart agriculture, some sensor nodes may be deployed beneath the soil or indoors, which is inconvenient to harvest the energy from the environmental resources. Thus, it is

Manuscript received February 8, 2020; revised April 27, 2020; accepted May 16, 2020. Date of publication May 22, 2020; date of current version March 5, 2021. This work was supported in part by the National Natural Science Foundation of China under Grants 61871348, in part by the University Key Laboratory of Advanced Wireless Communications of Guangdong Province, in part by the Project funded by China Postdoctoral Science Foundation under Grant 2019T120531, in part by the Science and Technology Development Fund, Macau SAR under Grant 0162/2019/A3, and in part by the Fundamental Research Funds for the Provincial Universities of Zhejiang under Grant RF-A2019001. Paper no. TII-20-0649. *(Corresponding author: Nan Zhao.)*

Weidang Lu, Xiaohan Xu, and Guoxing Huang are with the College of Information Engineering, Zhejiang University of Technology, Hangzhou 310023, China (e-mail: luweid@zjut.edu.cn; 18861121607@163.com; hgx05745@zjut.edu.cn).

Bo Li is with the School of Information Science and Engineering, Harbin Institute of Technology, Weihai 264209, China (e-mail: libo1983@hit.edu.cn).

Yuan Wu is with the State Key Laboratory of Internet of Things for Smart City, University of Macau, Macao 999078, China, and also with the Department of Computer and Information Science, University of Macau, Macao 999078, China (e-mail: yuanwu@um.edu.mo).

Nan Zhao is with the Key Laboratory of Intelligent Control and Optimization for Industrial Equipment of Ministry of Education, Dalian University of Technology, Dalian 116024, China (e-mail: zhaonan@dlut.edu.cn).

F. Richard Yu is with the Department of Systems and Computer Engineering, Carleton University, Ottawa, ON K1S 5B6, Canada (e-mail: richard.yu@carleton.ca).

Color versions of one or more of the figures in this article are available online at https://ieeexplore.ieee.org.

Digital Object Identifier 10.1109/TII.2020.2996672

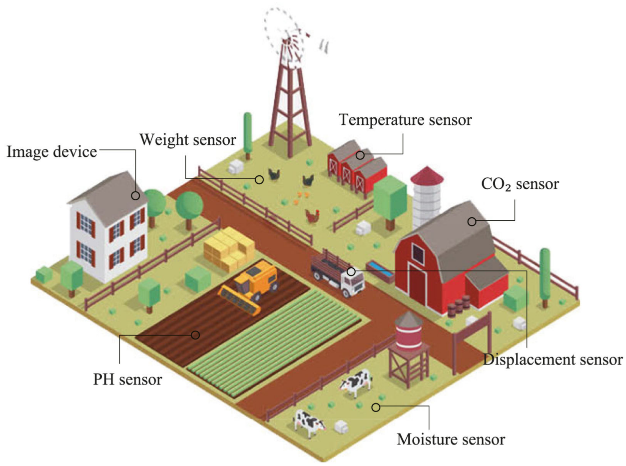


Fig. 1. Illustration of smart agriculture.

challenging to provide sustainable and reliable energy supply to massive low-power sensor nodes.

Different with the EH, wireless power transfer (WPT) is able to provide more stable and reliable energy supply to sensor nodes by using radio-frequency (RF) signals [15]–[25]. [17] proposed a WPT-based power allocation optimization strategy, in which the wireless sensor nodes are charged through receiving RF signals. As RF signals carry both energy and information, it makes possible to transfer information and energy simultaneously. Simultaneous wireless information and power transfer (SWIPT) is the technology proposed to harvest energy and decode information at the receiver from the same RF signals [26]–[35]. Time switching (TS) and power splitting (PS) are two realizable protocols proposed to realize SWIPT in the practical systems. In TS protocol, the receiver performs information decoding and energy harvesting in different time slots [26], [27]. In PS protocol, the power splitter divides the received power into two parts, one part for information decoding and the other for energy harvesting [28], [29]. It is envisioned that SWIPT can significantly improve the energy efficiency of the WSNs [30]–[35].

Motivated by the above-mentioned reasons, energy efficiency optimization in SWIPT-enabled WSNs for smart agriculture is studied in this article. With the target of maximizing the system energy efficiency, we jointly optimize the power allocation and pairing of subcarriers. To the authors best knowledge, this is the first work that considers the SWIPT-enabled WSNs for smart agriculture and studies the energy efficiency optimization problem in smart agriculture.

## II. Related Works

Energy efficiency optimization has been extensively studied in WPT communication system [18]–[25]. Song and Zheng [18] studied resource assignment optimization problem to maximize energy efficiency in wireless powered sensor networks with energy beamforming. Energy efficiency maximization problem is studied by jointly optimizing harvesting time and transmit power with nonorthogonal multiple access (NOMA) based wireless powered sensor networks [19]. Energy efficient resource allocation are studied in various WPT networks, e.g., multiple-antenna relay network [20], orthogonal frequency division multiple access (OFDMA) multicell network [21], mobile edge computing network [22], and device-to-device network [23]. Chang *et al.* [24] proposed a simple and effective ON–OFFkeying modulation method to achieve high energy efficiency operation in resonant WPT systems. Yang *et al.* [25] proposed an energy-efficient resource allocation scheme for a WPT-enabled multiuser massive multiple input multiple output (MIMO) system with imperfect channel estimation.

In SWIPT sensor networks, the sensor nodes are able to simultaneously perform energy harvesting and information decoding from the same received RF signal, which can improve the energy efficiency. Huang *et al.* [30] studied the tradeoff between system energy efficiency and throughput to satisfy the minimum transmission rate in SWIPT sensor networks. In [31], the energy efficiency maximization problem is studied in SWIPT-based IoT network, where IoT devices utilize PS protocol to coordinate the energy harvesting and information decoding processes through varying PS ratios of IoT devices and transmit power of distributed antenna ports. Tang *et al.* [32] studied the energy efficiency optimization for SWIPT-based MIMO two-way amplify-and-forward (AF) relaying networks through jointly designing the PS ratio and precoding metrics, in which relay forwards the source information by using the energy harvested from sources signals. Tang *et al.* [33] studied the energy efficiency optimization problem for SWIPT-based MIMO broadcast channels in IoT communication systems with TS receiver, where energy efficiency is maximized by optimizing the TS ratios and transmit covariance matrices. Lu *et al.* [34] proposed a joint spatial switching and antenna selection scheme for QoS-constrained energy efficiency optimization in a MIMO SWIPT system.

It is worth noting that in previous works, the energy efficiency optimization in SWIPT system is studied based on PS or TS protocol, which need to equip a power or time splitter at the receiver. However, due to the restrictions of the size and energy budget of sensor nodes, it is impractical to add a splitter at the sensor nodes. In this article, we studied the energy efficiency optimization in OFDM-based SWIPT-enabled WSNs for smart agriculture, in which the sensor nodes utilize different subcarriers to perform energy harvesting and information decoding. Then, the sensor nodes do not need to equip a splitter. We first proposed an architecture design of smart agriculture based on SWIPT-enabled WSNs and then studied the energy efficiency optimization problem in OFDM-based SWIPT enabled WSNs. With the target of maximizing the system energy efficiency, we jointly optimize the power allocation and pairing of subcarriers. Specifically, in the first phase, source sensor (SS) transmits information to relay sensor (RS) and destination sensor (DS). RS utilizes a part of the subcarriers to decode the information, and utilizes the remaining subcarriers to collect energy. DS utilizes all the subcarriers to receive the information. In the second phase, RS utilizes the energy collected in the first phase to send the

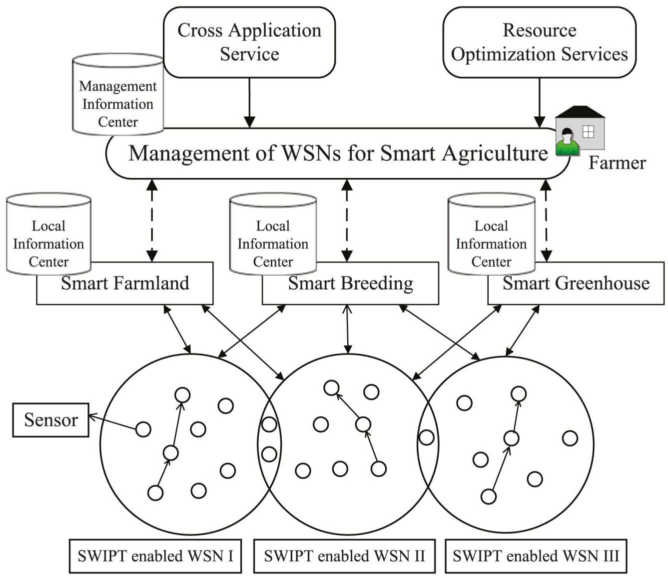


Fig. 2. Smart agriculture framework.

information to DS. The main contributions of this article are as follows.

1) We proposed an architecture design of smart agriculture based on SWIPT-enabled WSNs to achieve green communications.
2) An energy efficiency optimization problem for SWIPT-enabled WSNs is studied to maximize the system energy efficiency. In the optimization problem, we jointly optimize the subcarrier pairing and power allocation with the constraints of SS's transmission power and DS's target transmission rate.
3) Simulation results verify the performance of the energy efficiency for SWIPT-enabled WSNs of smart agriculture. It is shown that the proposed algorithm achieves larger system energy efficiency comparing with the other three algorithms.

The rest of this article is organized as follows. In Section III, we describe the smart agriculture architecture and the system model of OFDM-based SWIPT-enabled WSN. In Section IV, we present the problem formulation. Section V discusses the optimal solution to the objective function. In Section V, simulation results are given to illustrate the performance of the energy efficiency for SWIPT in WSNs by the algorithms proposed. Finally, Section VII concludes this article.

## III. Smart Agriculture Architecture and SWIPT Enabled WSNs System Model

### A. Architecture of Smart Agriculture

As shown in Fig. 2, the smart agriculture consists of three smart subsystems, which are smart farmland, smart breeding, and smart greenhouse. In each subsystem, the data collected by the sensors is transmitted to the subsystem through the WSNs. The local information center of the subsystem processes it and transmits it to the management information center of WSNs for smart agriculture. The management information center of WSNs for smart agriculture can optimize the data information to help farmers to make the best decisions.

In order to achieve large-scale smart agriculture, we require to deploy a good deal of WSNs, which will consume a lot of energy during the process of collecting and transmitting data. Since the limitation of the battery capacity of the sensor, we further proposed an energy efficiency optimization scheme in SWIPT-enabled WSNs for smart agriculture, in which the energy collected from the received RF signal is used for transmitting information to realize the target of green communication. Therefore, the remaining of the article is focused on the solution to the energy efficiency optimization of SWIPT-enabled WSNs for smart agriculture.

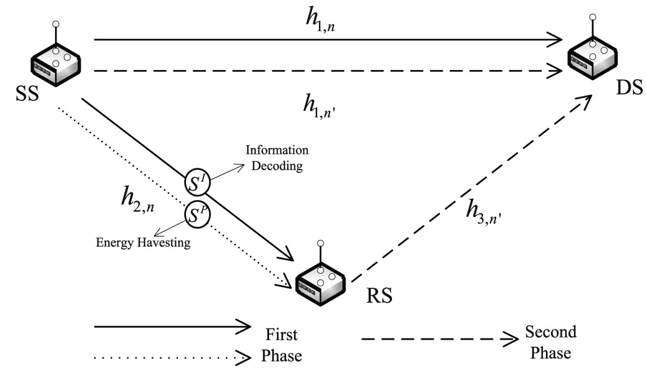


Fig. 3. SWIPT enabled on WSN.

### B. SWIPT-Enabled WSNs System Model

Fig. 3 shows a specific system model of SWIPT-enabled WSN, which consists of SS, RS, and DS. SS, RS, and DS are equipped with one single antenna, which work in half-duplex mode. The signal is OFDM modulated on $N$ subcarriers, and the set of subcarriers is denoted as $\mathcal{N} = \{1, 2, \ldots N\}$. We study slow fading that all the channel coefficients are presumed to be constant over multiple OFDM symbols. The channel is modeled as Rician fading, which is written as $h(k) = \sqrt{\frac{M}{M+1}}\widetilde{f} + \sqrt{\frac{1}{M+1}}\widehat{f}(k)$, where $M = 3$, $\widehat{f}(k)$ and $\widetilde{f}$ represent the Rayleigh fading and line of sight deterministic component, respectively. The channel gain of the subcarrier $n$ and $n'$ on SS→DS, SS→RS, and RS→DS links are expressed as $h_{1,n}$, $h_{1,n'}$, $h_{2,k}$, and $h_{3,n'}$, respectively.

The received signal on subcarrier $n$ and $n'$ at DS and RS will be corrupted by noise $n_{u,v}$, where $u \in \{1, 2, 3\}$ and $v \in \{n, n'\}$, which are modeled as an additive white Gaussian noise random variable with zero mean and variance $\sigma_{u,v}^2$, denoted as $n_{u,v} \sim \mathcal{CN}(0, \sigma_{u,v}^2)$. At the same time, we set the total transmission power of SS to $P$, and the target rate of DS to $R_T$.

## IV. Energy Efficiency Optimization Strategy

In the SWIPT-enabled WSN, the entire transmission process consists of two phases. In the first phase, SS sends information to RS and DS. RS uses subcarriers in $S^I$, which is a subset of $\mathcal{N}$, to decode the information. The transmit power over subcarrier $n \in S^I$ at SS is denoted as $p_{i,n}$. RS uses the subcarriers remained in $S^P$ to collect energy, where $S^I + S^P = \mathcal{N}$. The transmit power over subcarrier $n \in S^P$ is denoted as $p_{e,n}$.

Then, the rate received at RS is written as

$$R_{B,R} = \frac{1}{2} \sum_{n \in S^I} \ln \left( 1 + \frac{|h_{2,n}|^2 p_{i,n}}{\sigma_{2,n}^2} \right). \quad (1)$$

The energy collected by RS is written as

$$Q = \xi \sum_{n \in S^P} \left( p_{e,n} |h_{2,n}|^2 + \sigma_{2,n}^2 \right) \quad (2)$$

where $\xi$ is the energy conversion efficiency.

In the second phase, RS uses the energy collected in the first phase to AF the received information to DS through subcarrier pairing. Specifically, subcarriers in $G$, which is a subset of $\mathcal{N}$, are used to perform one-to-one subcarrier paring with the subcarriers in $S^I$ to forward the information, where $|G| = |S^I|$. The transmit power over subcarrier $n' \in G$ is denoted as $p_{r,n'}$.

Therefore, the rate received at DS with the help of RS is written as

$$R_{B,U}^R = \sum_{n \in S^I} \sum_{n'=1}^{N} \rho_{nn'} \ln \left( 1 + \delta_{n,n'} + \delta_{1,n} \right) \quad (3)$$

where $\delta_{n,n'} = \frac{|h_{2,n}|^2 |h_{3,n'}|^2 p_{i,n} p_{r,n'} / (\sigma_{3,n'}^2 \sigma_{2,n}^2)}{1 + |h_{2,n}|^2 p_{i,n} / \sigma_{2,n}^2 + |h_{3,n'}|^2 p_{r,n'} / \sigma_{3,n'}^2}$, $\delta_{1,n} = \frac{|h_{1,n}|^2 p_{i,n}}{\sigma_{1,n}^2}$, $\rho_{nn'}$ denotes the subcarrier pairing indicator. If the subcarrier $n$ used to receive information in the first phase is paired by the subcarrier $n'$ used to forward information in the second phase, then $\rho_{nn'} = 1$, otherwise $\rho_{nn'} = 0$. In the condition of large signal to noise ratio, $\delta_{n,n'}$ can be approximately [35] equal to $\delta_{n,n'} = \frac{|h_{2,n}|^2 |h_{3,n'}|^2 p_{i,n} p_{r,n'} / (\sigma_{3,n'}^2 \sigma_{2,n}^2)}{|h_{2,n}|^2 p_{i,n} / \sigma_{2,n}^2 + |h_{3,n'}|^2 p_{r,n'} / \sigma_{3,n'}^2}$.

As only a part of the subcarriers in $G$ are utilized by RS to forward the received information of SS to DS. Thus, the subcarriers remained in $\overline{G}$ can be used by SS to send information directly to DS, where $G + \overline{G} = \mathcal{N}$. The transmit power over subcarrier $n' \in \overline{G}$ is denoted as $p_{i,n'}$. Thus, the rate obtained at DS by direct transmission from SS in the second phase is written as

$$R_{B,U}^2 = \frac{1}{2} \sum_{n \in S^I} \sum_{n'=1}^{N} (1 - \rho_{nn'}) \ln \left( 1 + \frac{|h_{1,n'}|^2 p_{i,n'}}{\sigma_{1,n'}^2} \right). \quad (4)$$

Only the information transmitted by subcarriers in $S^I$ will be forwarded by RS to DS. However, the information transmitted by subcarriers in $S^P$ will be received for information decoding at DS through direct link in the first phase. Thus, the rate received at DS which transmitted from subcarriers in $S^P$ of SS transmission in the first phase can be written as

$$R_{B,U}^1 = \frac{1}{2} \sum_{n \in S^P} \ln \left( 1 + \frac{|h_{1,n}|^2 p_{e,n}}{\sigma_{1,n}^2} \right). \quad (5)$$

Thus, the total rate received at DS after two phases is written as

$$R_{\text{total}}(S, \rho, p) = R_{B,U}^R + R_{B,U}^1 + R_{B,U}^2 \quad (6)$$

where $R_{B,U}^R$ denotes the rate received at DS with the help of RS, $R_{B,U}^1$ denotes the rate received at DS which transmitted from subcarriers in $S^P$ of SS transmission in the first phase, and $R_{B,U}^2$ denotes the rate obtained at DS, which are transmitted from subcarriers in $\overline{G}$ of SS transmission in the second phase.

The total power consumption of the system during the two phases is written as

$$\begin{aligned} U_{\text{total}}(S, \rho, p) = {} & P_B + P_R + P_U + \sum_{n \in S^I} p_{i,n} + \sum_{n \in S^P} p_{e,n} \\ & + \sum_{n \in S^I} \sum_{n'=1}^{N} (1 - \rho_{nn'}) p_{i,n'} \\ & + \sum_{n \in S^I} \sum_{n'=1}^{N} \rho_{nn'} p_{r,n'} - Q \end{aligned} \quad (7)$$

where $P_B$, $P_R$, and $P_U$ are the fixed power consumption of the electronics at SS, RS, and DS, respectively.

Therefore, the system energy efficiency can be defined as the ratio between the received rate and the total power consumption [36], which can be written as

$$E_{\text{eff}}(S, \rho, p) = \frac{R_{\text{total}}(S, \rho, p)}{U_{\text{total}}(S, \rho, p)} \quad (8)$$

where $p = \{p_{i,n}, p_{e,n}, p_{r,n'}, p_{i,n'}\}$, $\rho = \{\rho_{nn'}\}$ and $S = \{S^P, S^I\}$.

In order to maximize the system energy efficiency, the subcarrier set $S$, the subcarrier pairing $\rho$, and the subcarrier power allocation $p$ are jointly optimized. The optimization problem is written as

$$\max_{\{S, \rho, p\}} E_{eff}(S, \rho, p) \quad (9)$$

subject to

$$C1: R_{\text{total}}(S, \rho, p) \geq R_T$$

$$C2: P_B + P_R + P_U + \sum_{n \in S^I} p_{i,n} + \sum_{n \in S^P} p_{e,n} \leq P$$

$$C3: \sum_{n \in S^I} \sum_{n'=1}^{N} \rho_{nn'} p_{r,n'} \leq Q$$

$$C4: \sum_{n \in S^I} \sum_{n'=1}^{N} (1 - \rho_{nn'}) p_{i,n'} \leq P$$

$$C5: S^I + S^P = \mathbf{N}$$

$$C6: S^I \cap S^P = \emptyset$$

where $C1$ represents the limitation of DS's target transmission rate, $C2$ and $C4$ represent that the power consumed by the system cannot exceed the total transmission power $P$, $C3$ represents that the power transmitted at RS in the second phase to forward information should be smaller than the energy collected in the first phase, $C5$ and $C6$ represent the subcarrier set constraints.

Let $q^*$ denote the system maximum energy efficiency, which is written as

$$q^* = \frac{R_{\text{total}}(S^*, \rho^*, p^*)}{U_{\text{total}}(S^*, \rho^*, p^*)} = \max_{\{S,\rho,p\}} \frac{R_{\text{total}}(S, \rho, p)}{U_{\text{total}}(S, \rho, p)}. \tag{10}$$

The maximum energy efficiency $q^*$ can only be obtained [36] when $\max_{S,\rho,p} R_{\text{total}}(S, \rho, p) - q^* U_{\text{total}}(S, \rho, p) = R_{\text{total}}(S^*, \rho^*, p^*) - q^* U_{\text{total}}(S^*, \rho^*, p^*) = 0$.

Due to the fractional form of the energy efficiency representation of (9), the optimal solution is hard to be obtained directly. Through utilizing $q$, (9) can be transformed into a new objective function

$$\max_{\{S,\rho,p\}} R_{\text{total}}(S, \rho, p) - qU_{\text{total}}(S, \rho, p) \tag{11}$$

subject to

$$C1, C2, C3, C4, C5, C6.$$

## V. Optimal Solution

The optimization objective function is a nonconvex optimization problem. When the subcarriers number is large and "time-sharing" condition is satisfied, Lagrange dual function and Dinkelbach iterative algorithm can be utilized to solve this problem [37].

The Lagrange dual function of the optimization problem in (2) can be written as

$$g(\beta) = \max_{\{S,\rho,p\}} L(S, \rho, p) \tag{12}$$

where $L(S, \rho, p)$ is written as

$$\begin{aligned} L(S, \rho, p) &= R_{\text{total}}(S, \rho, p) - qU_{\text{total}}(S, \rho, p) \\ &\quad + \beta_1 \left(R_{\text{total}}(S, \rho, p) - R_T\right) \\ &\quad + \beta_2 \left(P - P_B - P_R - P_U - \sum_{n\in S^I} p_{i,n} - \sum_{n\in S^P} p_{e,n}\right) \\ &\quad + \beta_3 \left(Q - \sum_{n\in S^I}\sum_{n'=1}^{N} \rho_{nn'} p_{r,n'}\right) \\ &\quad + \beta_4 \left(P - \sum_{n\in S^I}\sum_{n'=1}^{N} (1-\rho_{nn'}) p_{i,n'}\right) \end{aligned} \tag{13}$$

where $\boldsymbol{\beta} = (\beta_1, \beta_2, \beta_3, \beta_4)$ is the vector of dual variables.

The dual optimization problem can be written as

$$\min_{\beta} g(\beta) \tag{14}$$

subject to $\beta \geq 0$.

The optimal dual variables $\boldsymbol{\beta}^* = (\beta_1^*, \beta_2^*, \beta_3^*, \beta_4^*)$ can be obtained by utilizing subgradient method. The subgradient of $g(\beta)$ is written as

$$\begin{aligned} \Delta\beta_1 &= R_{\text{total}}(S, \rho, p) - R_T \\ \Delta\beta_2 &= P - P_B - P_R - P_U - \sum_{n\in S^I} p_{i,n} - \sum_{n\in S^P} p_{e,n} \\ \Delta\beta_3 &= Q - \sum_{n\in S^I}\sum_{n'=1}^{N} \rho_{nn'} p_{r,n'} \\ \Delta\beta_4 &= P - \sum_{n\in S^I}\sum_{n'=1}^{N} (1-\rho_{nn'}) p_{i,n'}. \end{aligned} \tag{15}$$

Update iteratively by $\beta^{(t+1)} = (\beta^{(t)} + \eta^{(t)}\Delta\beta)$, where $\eta^{(t)}$ represents the iteration step size, $t$ represents the number of iterations, and $\Delta\beta = (\Delta\beta_1, \Delta\beta_2, \Delta\beta_1, \Delta\beta_4)$. When convergence is reached, the optimal dual variables can be obtained. The computational complexity of this method is given by $O(V^\alpha)$, where $\alpha$ is a non-negative integer and $V$ is the number of dual variables.

With given $\boldsymbol{\beta}$, the optimal $\{S, \rho, p\}$ can be obtained through the following three steps.

### A. Obtaining Optimal $p$ With Fixed $S$ and $\rho$

To facilitate the calculation, we introduce the variables $\gamma_{1,n} = \frac{|h_{1,n}|^2}{\sigma_{1,n}^2}, \gamma_{2,n} = \frac{|h_{2,n}|^2}{\sigma_{2,n}^2}, \gamma_{1,n'} = \frac{|h_{1,n'}|^2}{\sigma_{1,n'}^2}, \gamma_{3,n'} = \frac{|h_{3,n'}|^2}{\sigma_{3,n'}^2}$.

The partial derivatives of $L(S, \rho, p)$ with $p_{e,n}, p_{i,n}, p_{i,n'}$, and $p_{r,n'}$ can be written as

$$\begin{aligned} \frac{\partial L}{\partial p_{e,n}} &= \frac{(1+\beta_1)\gamma_{1,n}}{2(1+p_{e,n}\gamma_{1,n})} - (q+\beta_2) + \xi\sigma_{2,n}^2\gamma_{2,n}(\beta_3+q) \\ \frac{\partial L}{\partial p_{i,n'}} &= \frac{(1+\beta_1)\gamma_{1,n'}}{2(1+p_{i,n'}\gamma_{1,n'})} - (q+\beta_4) \\ \frac{\partial L}{\partial p_{i,n}} &= \frac{(1+\beta_1)\alpha_1}{2\alpha_2} - (q+\beta_2) \\ \frac{\partial L}{\partial p_{r,n'}} &= \frac{(1+\beta_1)p_{i,n'}^2\gamma_{2,n}^2\gamma_{3,n'}}{2\alpha_2} - (q+\beta_3) \end{aligned} \tag{16}$$

where $\alpha_1 = \gamma_{1,n}(p_{i,n}\gamma_{2,n} + p_{r,n'}\gamma_{3,n'})^2 + p_{r,n'}^2\gamma_{3,n'}^2\gamma_{2,n}$ and $\alpha_2 = ((1+p_{i,n}\gamma_{1,n})(p_{i,n}\gamma_{2,n} + p_{r,n'}\gamma_{3,n'}) + p_{i,n}\gamma_{2,n}p_{r,n'}\gamma_{3,n'})(p_{i,n}\gamma_{2,n} + p_{r,n'}\gamma_{3,n'})$.

The optimal $p_{e,n}, p_{i,n}, p_{i,n'}$, and $p_{r,n'}$ can be obtained through the Karush Kuhn Tucher (KKT) conditions by equating the partial derivative of the Lagrangian to zero.

Equating $\frac{\partial L}{\partial p_{e,n}}$ and $\frac{\partial L}{\partial p_{i,n'}}$ to zero, we can obtain

$$\begin{aligned} p_{e,n}^* &= \left(\frac{1+\beta_1}{2\left((q+\beta_2) - \xi\sigma_{2,n}^2\gamma_{2,n}(\beta_3+q)\right)} - \frac{1}{\gamma_{1,n}}\right)^+ \\ p_{i,n'}^* &= \left(\frac{1+\beta_1}{2(q+\beta_4)} - \frac{1}{\gamma_{1,n'}}\right)^+. \end{aligned} \tag{17}$$

Equating $\frac{\partial L}{\partial p_{i,n}}$ and $\frac{\partial L}{\partial p_{r,n'}}$ to zero, we can obtain

$$\frac{\gamma_{1,n}(p_{i,n}\gamma_{2,n} + p_{r,n'}\gamma_{3,n'})^2 + p_{r,n'}^2\gamma_{3,n'}^2\gamma_{2,n}}{q+\beta_2} = \frac{p_{i,n'}^2\gamma_{2,n}^2\gamma_{3,n'}}{q+\beta_3}. \tag{18}$$

By further simplification, we can obtain

$$Ap_{i,n}^2 = Bp_{r,n'}^2 + 2(q+\beta_3)\gamma_{1,n}\gamma_{2,n}\gamma_{3,n'}p_{i,n}p_{r,n'} \tag{19}$$

where $A = (q+\beta_2)\gamma_{2,n}^2\gamma_{3,n'} - (q+\beta_3)\gamma_{1,n}\gamma_{2,n}^2$ and $B = (q+\beta_3)\gamma_{1,n}\gamma_{3,n'}^2 + (q+\beta_3)\gamma_{3,n'}^2\gamma_{2,n}$.

Assume $p_{i,n} = t_{n,n'}p_{r,n'}$. Substituting it into (19), we can obtain

$$Ct_{n,n'}^2 - Dt_{n,n'} - (q+\beta_3)\gamma_{3,n'}^2(\gamma_{1,n}+\gamma_{2,n}) = 0 \tag{20}$$

where $C = \gamma_{2,n}^2((q+\beta_2)\gamma_{3,n'} - (q+\beta_3)\gamma_{1,n})$ and $D = 2(q+\beta_3)\gamma_{1,n}\gamma_{2,n}\gamma_{3,n'}$.

From (20), we can obtain

$$\Delta = E\left((q+\beta_2)(\gamma_{1,n}\gamma_{3,n'} + \gamma_{2,n}\gamma_{3,n'}) - (q+\beta_3)\gamma_{1,n}\gamma_{2,n}\right) \tag{21}$$

where $E = 4(q+\beta_3)\gamma_{2,n}^2\gamma_{3,n'}^2$.

Only when $\Delta \geq 0$, (20) can have real roots. Then, we can obtain $(q+\beta_2)(\gamma_{1,n}\gamma_{3,n'} + \gamma_{2,n}\gamma_{3,n'}) \geq (q+\beta_3)\gamma_{1,n}\gamma_{2,n}$. Since $t_{n,n'}$ is larger than 0, then we can obtain

$$t_{n,n'} = \frac{2(q+\beta_3)\gamma_{1,n}\gamma_{2,n}\gamma_{3,n'} + \sqrt{\Delta}}{2\gamma_{2,n}^2\left((q+\beta_2)\gamma_{3,n'} - (q+\beta_3)\gamma_{1,n}\right)}. \tag{22}$$

Substituting (22) into $\dfrac{\partial L}{\partial p_{i,n}} = 0$, we can obtain

$$p_{i,n}^* = \left(\frac{\omega_1 t_{n,n'} - 2(q+\beta_3)t_{n,n'}(\gamma_{2,n}t_{n,n'} + \gamma_{3,n'})^2}{2(q+\beta_3)\omega_2}\right)^+$$
$$p_{r,n'}^* = \left(\frac{\omega_1 - 2(q+\beta_3)(\gamma_{2,n}t_{n,n'} + \gamma_{3,n'})^2}{2(q+\beta_3)\omega_2}\right)^+ \tag{23}$$

where $\omega_1 = \gamma_{2,n}^2\gamma_{3,n'}t_{n,n'}^2$ and $\omega_2 = (\gamma_{2,n}t_{n,n'} + \gamma_{3,n'})(\gamma_{1,n}\gamma_{2,n}t_{n,n'}^2 + \gamma_{3,n'}(\gamma_{1,n}+\gamma_{2,n})t_{n,n'})$.

## B. Obtaining Optimal $\rho$ for Fixed $S$

Substituting (17) and (23) into (13), $L(S,\rho,p)$ can be rewritten as

$$\begin{aligned} L(S,\rho,p) = &\sum_{n\in S^I}\sum_{n'=1}^{N}\rho_{nn'}E_{n,n'} + \sum_{n\in S^I}\omega_4 + \sum_{n=1}^{N}\omega_5 \\ &+ \sum_{n'=1}^{N}\omega_6 - (q+\beta_2)(P_B+P_R+P_U) \\ &- \beta_1 R_T + (\beta_2+\beta_4)P \end{aligned} \tag{24}$$

where $\omega_4 = (q+\beta_2)(p_{e,n}^* - p_{i,n}^*) - \frac{1+\beta_1}{2}\ln(1+p_{e,n}^*\gamma_{1,n}) - \xi(\beta_3+q)(p_{e,n}^*\gamma_{2,n} + \sigma_{2,n}^2)$, $\omega_5 = \frac{1+\beta_1}{2}\ln(1+p_{e,n}^*\gamma_{1,n}) + \xi(\beta_3+q)(p_{e,n}^*\sigma_{2,n}^2\gamma_{2,n} + \sigma_{2,n}^2) - (q+\beta_2)p_{e,n}^*$, $\omega_6 = \frac{1+\beta_1}{2}\ln(1+p_{i,n'}^*\gamma_{1,n'}) - (q+\beta_4)p_{i,n'}^*$, and $E_{n,n'} = \frac{1+\beta_1}{2}\ln(1+p_{i,n}^*\gamma_{1,n} + \frac{p_{i,n}^*\gamma_{2,n}p_{r,n'}^*\gamma_{3,n'}}{p_{i,n}^*\gamma_{2,n}+p_{r,n'}^*\gamma_{3,n'}}) - \frac{1+\beta_1}{2}\ln(1+p_{i,n'}^*\gamma_{1,n'}) + (q+\beta_4)p_{i,n'}^* - (\beta_3+q)p_{r,n'}^*$.

Obviously, $\rho_{nn'}$ is only related to $E_{n,n'}$. Therefore, the optimal subcarrier $n'$, which will be paired with $n$ can be obtained by finding the largest value of $E_{n,n'}$, which can be given by

$$n'^* = \arg\max_{n'} E_{n,n'}. \tag{25}$$

**Algorithm 1:** The Algorithm to Solve the Optimization Problem.

1: **initialize** the dual variables $\beta_1, \beta_2, \beta_3$, and $\beta_4$.
2: **repeat**
3: Compute the optimal power allocation $p_{e,n}^*, p_{i,n}^*, p_{i,n'}^*$, and $p_{r,n'}^*$ defined in (17) and (23).
4: Compute the optimal subcarrier paring $\rho_{nn'}^*$ defined in (25) and (26).
5: Compute the optimal subcarrier allocation sets $\mathcal{S}^{I*}$ and $\mathcal{S}^{P*}$ defined in (28) and (29).
6: Update $\beta_1, \beta_2, \beta_3$, and $\beta_4$ by using the subgradient method with the subgradients defined in (15).
7: **until** $\beta_1, \beta_2, \beta_3$, and $\beta_4$ converge.

Then, for each $n$, $n \in S^I$ form a pair $(n, n'^*)$. The optimal subcarrier paring $\rho_{nn'}^*$ are the given by

$$\begin{aligned} &\rho_{nn'^*}^* = 1 \\ &\rho_{nn'}^* = 0 \quad \forall n' \neq n'^*. \end{aligned} \tag{26}$$

The computational complexity of above subcarrier pairing is given by $O(NK)$, where $K = |G|$.

## C. Obtaining the optimal $S$

After obtaining the optimal subcarrier pairing $\rho_{nn'}^*$, (24) can be rewritten as

$$\begin{aligned} L(S,\rho,p) = &\sum_{n\in S^I}F_{n,n'} + \sum_{n=1}^{N}\omega_5 + \sum_{n'=1}^{N}\omega_6 \\ &- (q+\beta_2)(P_B+P_R+P_U) \\ &- \beta_1 R_T + (\beta_2+\beta_4)P \end{aligned} \tag{27}$$

where $F_{n,n'} = E_{n,n'} + (q+\beta_2)(p_{e,n}^* - p_{i,n}^*) - \frac{1+\beta_1}{2}\ln(1+p_{e,n}^*\gamma_{1,n}) - \xi(\beta_3+q)(p_{e,n}^*\sigma_{2,n}^2\gamma_{2,n} + \sigma_{2,n}^2)$.

It can be seen from (27) that the subcarrier set $S^I$ is only related to $F_{n,n'}$. Thus, the optimal subcarrier set $S^{I^*}$ can be written as

$$S^{I^*} = \arg\max_{S^I}\sum_{k\in S^I}F_{n,n'^*}. \tag{28}$$

It is easy to find that all these $n$'s ($n \in \mathcal{N}$) make $F_{n,n'^*}$ positive form $S^{I^*}$. The involved computational complexity is given by $O(N)$. Then, optimal $S^{P^*}$ can be written as

$$S^{P^*} = \mathcal{N} - S^{I^*}. \tag{29}$$

We obtain the optimal solution in one Dinkelbach iteration. The above algorithm to solve (11) is concludes in Algorithm 1 [37].

We can obtain the maximum energy efficiency through iterations, and the Dinkelbach Iterative Algorithm is shown in Algorithm 2 [37]. The involved computational complexity is given by $O(L)$, where $L$ is the iterations for the convergence of the Dinkelbach iteration algorithm.

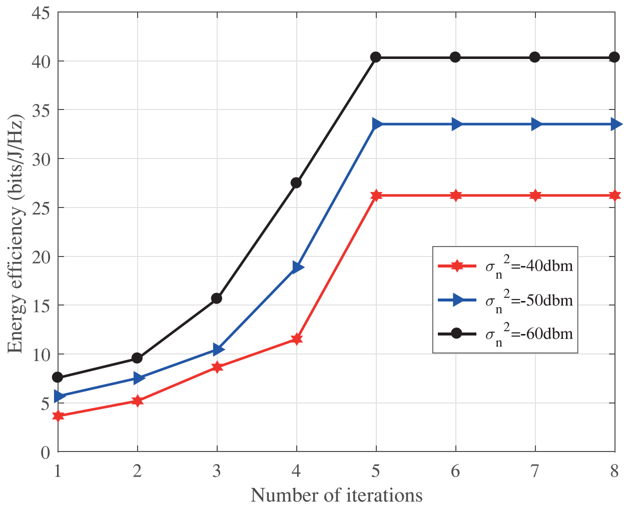


Fig. 4. Energy efficiency versus iterations.

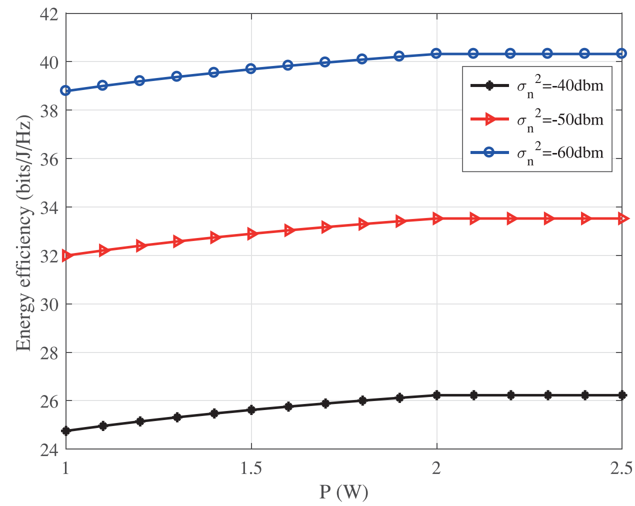


Fig. 5. Energy efficiency versus $P$.

**Algorithm 2:** The Algorithm of Dinkelbach Iterative.

**initialize** the maximum number of iterations $T$ and maximum error $\tau$.
**set** $q = 0, t = 0$.
**repeat**
$\{S, \rho, p\}$ obtained from Algorithm 1.
**if**
$R_{\text{total}}(S, \rho, p) - qU_{\text{total}}(S, \rho, p) \le \tau$.
return $\{S^*, \rho^*, p^*\} = \{S, \rho, p\}$, $q = \frac{R_{\text{total}}(S,\rho,p)}{U_{\text{total}}(S,\rho,p)}$.
**else**
$q = \frac{R_{\text{total}}(S,\rho,p)}{U_{\text{total}}(S,\rho,p)}$, $t = t + 1$.
**end**
**until** $R_{\text{total}}(S, \rho, p) - qU_{\text{total}}(S, \rho, p) \le \tau$ is true.

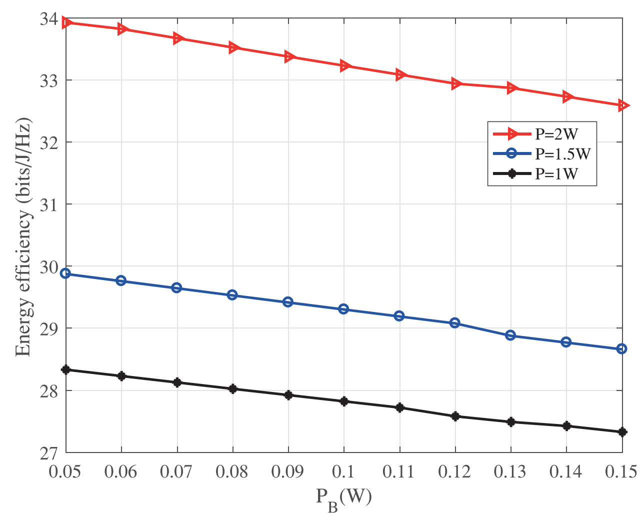


Fig. 6. Energy efficiency versus $P_B$.

## VI. Simulation Results

In this section, the energy efficiency of our proposed algorithm is evaluated by simulation results. The number of subcarriers is $N = 32$. For simplicity, we set the energy conversion efficiency $\xi = 1$, $\sigma_{u,v}^2 = \sigma_n^2$.

Fig. 4 illustrates the convergence of the proposed algorithm with the number of iterations at different noise powers when $P = 2$W. From Fig. 4, we can find that the energy efficiency will be converged after five iterations. We can also find from Fig. 4 that the system energy efficiency becomes larger with the smaller noise power. It is because that smaller noise power will lead to larger rate and smaller power, which obtains larger energy efficiency.

Fig. 5 shows the system energy efficiency versus the total transmission power $P$ of SS with different noise powers. From Fig. 5, we can find that the system energy efficiency improves with the total transmission power $P$ gradually increasing from 1.0 to 2.0 W, which is because RS can collect more energy when $P$ becomes larger. When $P = 2.0$ W, the system energy efficiency achieves its maximum value. Then, the energy efficiency of the system is no longer changed when $P$ increases. It is because that when the constraint of the target rate is reached at DS, SS will not increase its power to transmit the information, which result the rate at DS and the total power consumption with fixed values.

Fig. 6 shows the effect of the power consumption of the electronics at SS on the system energy efficiency with different total transmission power $P$. We can observe from Fig. 6 that the system energy efficiency becomes smaller with small total transmission power $P$, which is consistent with the result in Figs. 5. In Fig. 6, we can also find that the system energy efficiency decreases with the power consumption of the electronics at SS. In (7), it is easy to find that the total power consumption increases with the power consumption of the electronics at SS, which results in the decreasing of the system energy efficiency.

Fig. 7 and 8 show the allocation of subcarriers and power in the first phase and second phase when $P = 2$ W and $R_T = 10$ b/s, respectively. In the first phase, the number of subcarriers used for information decoding, $|S^I|$, is small. This is because that

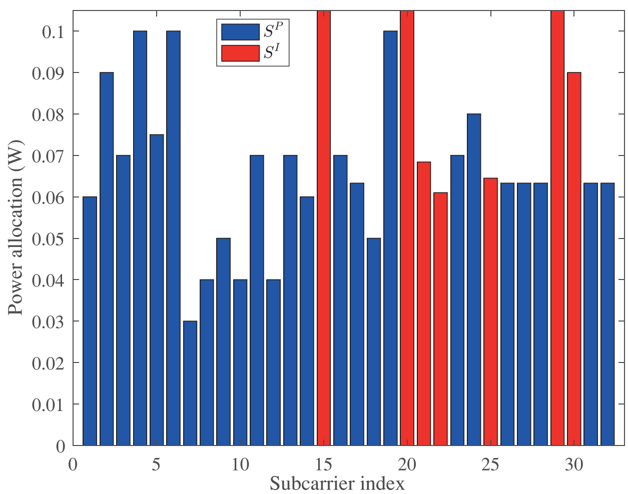


Fig. 7. Subcarrier and power allocation in the first phase.

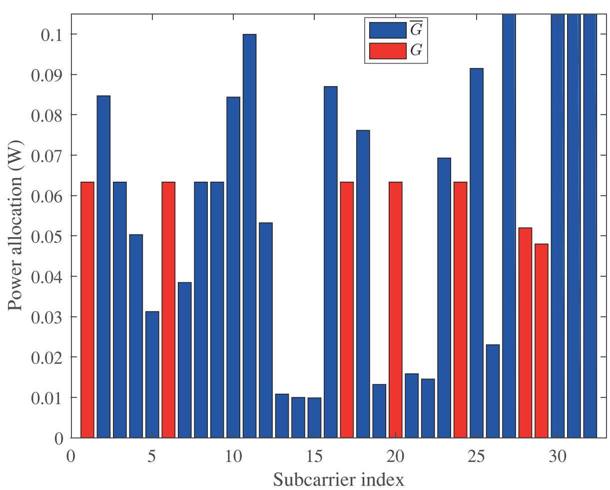


Fig. 8. Subcarrier and power allocation in the second phase.

when the target of DS's transmission rate $R_T$ is small, only a small number of subcarriers used to decode information is able to reach $R_T$. For purpose of increasing the system energy efficiency, most of the subcarriers are utilized to collect energy to reduce the power consumption. In the second phase, since the subcarriers are one-to-one paired, the number of subcarriers used by the RS in the second phase for forwarding the information equals to the number of subcarriers for decoding information in the first phase, i.e., $|G| = |S^I|$.

In Fig. 9, to demonstrate the superiority of the proposed resource allocation strategy, we contrasted the performance of our proposed algorithm with the following three suboptimal algorithms.

Algorithm 1: The subcarriers are sorted in descending order on the basis of the channel gain in two phases. Then, the subcarrier with the best channel gain in the first phase is paired by the subcarriers with the best channel gain in second phase, until all subcarriers in $S^I$ are paired in order. The method of subcarriers and power allocation is the same as the method that proposed in this article.

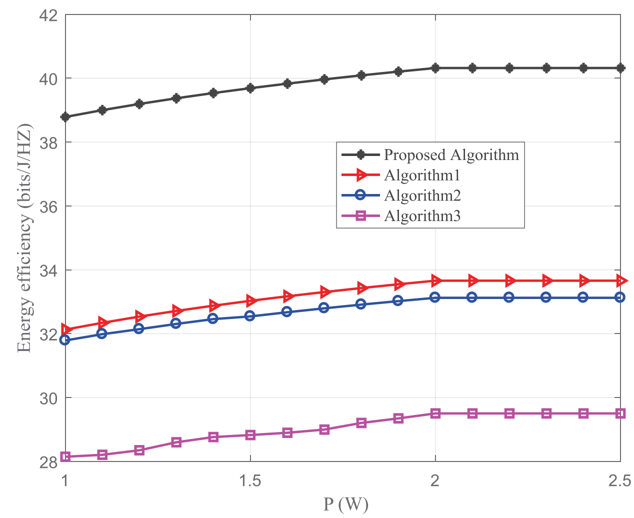


Fig. 9. Comparison of energy efficiency of different algorithms.

Algorithm 2: The method of subcarriers' allocation and subcarriers' pairing are the same as the method in our proposed algorithm. However, the power in the first phase is medially allocated, and the power in the second time slot is allocated according water filling approach.

Algorithm 3: The SS subcarriers are randomly paired with the RS subcarriers. The power in the first phase and second phase are allocated according to the water filling approach. The subcarrier allocation method is the same as the method proposed in this article.

From Fig. 9, we can observe that our proposed algorithm achieves preferable performance than Algorithm 1, Algorithm 2, and Algorithm 3. The performance of Algorithm 1 is superior to Algorithm 2. It is due to the subcarrier paring in Algorithm 1 and the power allocation in Algorithm 2 are not optimized, which results the performance degradation. The performance of Algorithm 1 and Algorithm 2 are superior to Algorithm 3. It is due to the subcarrier paring in Algorithm 3 are randomly paired, which will seriously degrade the performance. The advantage of the system energy efficiency of our proposed algorithm comparing with Algorithm 1, Algorithm 2, and Algorithm 3 can verify the superiority of subcarrier pairing and power allocation proposed in this article.

## VII. Conclusion

In this article, we first proposed an architecture design of smart agriculture based on SWIPT-enabled WSNs. Then, an energy efficiency optimization scheme for SWIPT-enabled WSNs was studied to achieve green communication. The communication process was divided into two phases. In the first phase, SS sent information to RS and DS. RS used a part of the subcarriers to decode the information, and used the remaining subcarriers to collect energy. DS used all the subcarriers to receive the information. In the second phase, RS used the energy collected in the first phase to forward the information to DS. Maximum energy efficiency was achieved by jointly optimizing the power allocation for transmitting information and energy, subcarriers pairing, and allocation. The simulation results verify that the proposed algorithm can improve the system energy efficiency through comparing with the two benchmark algorithms. In future work, we will extend our work into multiple sensors nodes scene by considering interference problem, sensor nodes selection, and rout optimization.

## REFERENCES


[1] O. Elijah, T. A. Rahman, I. Orikumhi, C. Y. Leow, and M. N. Hindia, "An overview of Internet of Things (IoT) and data analytics in agriculture: Benefits and challenges," *IEEE Internet Things J.*, vol. 5, no. 5, pp. 3758–3773, Oct. 2018.

[2] X. Liu, X. Zhai, W. Lu, C. Wu, "QoS-guarantee resource allocation for multibeam satellite industrial Internet of Things with NOMA," *IEEE Trans. Ind. Informat.*, Nov. 2019, doi: 10.1109/TII.2019.2951728.

[3] X. Liu, M. Jia, X. Zhang, and W. Lu, "A novel multichannel Internet of Things based on dynamic spectrum sharing in 5G communication," *IEEE Internet Things J.*, vol. 6, no. 4, pp. 5962–5970, Jun. 2018.

[4] N. Ahmed, D. De, and I. Hussain, "Internet of Things (IoT) for smart precision agriculture and farming in rural areas,"*IEEE Internet Things J.*, vol. 5, no. 6, pp. 4890–4899, Dec. 2018.

[5] M. S. Farooq, S. Riaz, A. Abid, K. Abid, and M. A. Naeem, "A survey on the role of IoT in agriculture for the implementation of smart farming," *IEEE Access*, vol. 7, pp. 156237–156271, 2019.

[6] Agrawal, H. Dhall, R. Iyer, K. Chetlapalli, Vijayalakshmi, "An improved energy efficient system for IoT enabled precision agriculture," *J. Ambient Intell. Humaniz. Comput.*, May 2019, doi: 10.1007/s12652-019-01359-2.

[7] M. Lafont, S. Dupont, P. Cousin, A. Vallauri, and C. Dupont, "Back to the future: IoT to improve aquaculture : Real-time monitoring and algorithmic prediction of water parameters for aquaculture needs," in *Proc. Global IoT Summit*, Aarhus, Denmark, 2019, pp. 1–6.

[8] R. Li, X. Sha, and K. Lin, "Smart greenhouse: A real-time mobile intelligent monitoring system based on WSN," in *Proc. Int. Wireless Commun. Mobile Comput. Conf.*, Nicosia, Cyprus, 2014, pp. 1152–1156.

[9] T. Cao-hoang and C. N. Duy, "Environment monitoring system for agricultural application based on wireless sensor network," in *Proc. 7th Int. Conf. Inf. Sci. Technol.*, Da Nang, Vietnam, 2017, pp. 99–102.

[10] M. Roopaei, P. Rad, and K. R. Choo, "Cloud of things in smart agriculture: Intelligent irrigation monitoring by thermal imaging," *IEEE Cloud Comput.*, vol. 4, no. 1, pp. 10–15, Jan./Feb. 2017.

[11] Y. Zhang, H. Gao, S. Cheng, and J. Li, "An efficient EH-WSN energy management mechanism," *Tsinghua Sci. Technol.*, vol. 23, no. 4, pp. 406–418, Aug. 2018.

[12] L. P. Qian, G. Feng, and V. C. M. Leung, "Optimal transmission policies for relay communication networks with ambient energy harvesting relays," *IEEE J. Sel. Areas Commun.*, vol. 34, no. 12, pp. 3754–3768, Dec. 2016.

[13] H. Sharma, A. Haque, and Z. Jaffery, "Maximization of wireless sensor network lifetime using solar energy harvesting for smart agriculture monitoring," *Ad Hoc Netw.*, vol. 94, pp. 1–14, Nov. 2019.

[14] Y. Tan and S. Panda, "Optimized wind energy harvesting system using resistance emulator and active rectifier for wireless sensor nodes," *IEEE Trans. Power Electron.*, vol. 26, no. 1, pp. 38–50, Jan. 2011.

[15] Y. Huang and B. Clerckx, "Waveform design for wireless power transfer with limited feedback," *IEEE Trans. Wireless Commun.*, vol. 17, no. 1, pp. 415–429, Jan. 2018.

[16] L. Qian, Y. Wu, B. Ji, and S. Shen, "Optimal ADMM-based spectrum and power allocation for heterogeneous small-cell networks with hybrid energy supplies," *IEEE Trans. Mobile Comput.*, Oct. 2019, doi: 10.1109/TMC.2019.2948014.

[17] L. Sun, L. Wan, K. Liu, and X. Wang, "Cooperative-evolution-based WPT resource allocation for large-scale cognitive industrial IOT," *IEEE Trans. Ind. Informat.*, Dec. 2019, doi: 10.1109/TII.2019.2961659.

[18] T. Liu, X. Qu, F. Yin, and Y. Chen, "Energy efficiency maximization for wirelessly powered sensor networks with energy beamforming," *IEEE Commun. Lett.*, vol. 23, no. 12, pp. 2311–2315, Dec. 2019.

[19] M. Song and M. Zheng, "Energy efficiency optimization for wireless powered sensor networks with nonorthogonal multiple access," *IEEE Sensors Lett.*, vol. 2, no. 1, pp. 1–4, Mar. 2018.

[20] Z. Chang, X. Hou, T. Ristaniemi, and Z. Han, "Secure and energy-efficient resource allocation for wireless power enabled full-/half-Duplex multiple-antenna relay systems," *IEEE Veh. Technol.*, vol. 66, no. 12, pp. 11208–11219, Dec. 2017.

[21] Z. Chang, Z. Wang, X. Guo, C. Yang, Z. Han, and T. Ristaniemi, "Distributed resource allocation for energy efficiency in OFDMA multicell networks with wireless power transfer," *IEEE J. Sel. Areas Commun.*, vol. 37, no. 2, pp. 345–356, Feb. 2019.

[22] L. Ji and S. Guo, "Energy-efficient cooperative resource allocation in wireless powered mobile edge computing," *IEEE Internet Things J.*, vol. 6, no. 3, pp. 4744–4754, Jun. 2019.

[23] H. Dai, Y. Huang, C. Li, S. Li, and L. Yang, "Energy-efficient resource allocation for device-to-device communication with WPT," *IET Comm.*, vol. 11, no. 3, pp. 326–324, Feb. 2017.

[24] W. Zhong and S. Hui, "Maximum energy efficiency operation of series-series resonant wireless power transfer systems using on-off keying modulation," *IEEE Trans. Power Electron.*, vol. 33, no. 4, pp. 3595–3603, Apr. 2018.

[25] Z. Chang, Z. Wang, X. Guo, Z. Han, and T. Ristaniemi, "Energy-efficient resource allocation for wireless powered massive MIMO system with imperfect CSI," *IEEE Trans. Green Commun. Netw.*, vol. 1, no. 2, pp. 121–130, Jun. 2017.

[26] W. Yang, W. Mou, X. Xu, W. Yang, and Y. Cai, "Energy effciency analysis and enhancement for secure transmission in SWIPT systems exploiting full duplex techniques," *IET Commun.*, vol. 10, no. 14, pp. 1712–1720, Sep. 2016.

[27] Q. Sun, L. Li, and J. Mao, "Simultaneous information and power transfer scheme for energy effcient MIMO systems," *IEEE Commun. Lett.*, vol. 18, no. 4, pp. 600–603, Apr. 2014.

[28] Y. Huang, M. Liu, and Y. Liu, "Energy-effcient SWIPT in IoT distributed antenna systems," *IEEE Internet Things J.*, vol. 5, no. 4, pp. 2646–2656, Aug. 2018.

[29] S. Guo, Y. Shi, Y. Yang, and B. Xiao, "Energy effciency maximization in mobile wireless energy harvesting sensor networks," *IEEE Trans. Mobile Comput.*, vol. 17, no. 7, pp. 1524–1537, Jul. 2018.

[30] S. Guo, Y. Shi, Y. Yang, and B. Xiao, "Energy efficiency maximization in mobile wireless energy harvesting sensor networks," *IEEE Trans. Mobile Comput.*, vol. 17, no. 7, pp. 1524–1537, Jul. 2018.

[31] Y. Huang, M. Liu, and Y. Liu, "Energy-efficient SWIPT in IoT distributed antenna systems," *IEEE Internet Things J.*, vol. 5, no. 4, pp. 2646–2656, Aug. 2018.

[32] X. Zhou and Q. Li, "Energy efficiency for SWIPT in MIMO two-way amplify-and-forward relay networks," *IEEE Trans. Veh. Technol.*, vol. 67, no. 6, pp. 4910–4924, Jun. 2018.

[33] J. Tang, D. So, N. Zhao, A. Shojaeifard, and K. Wang, "Energy efficiency optimization with SWIPT in MIMO broadcast channels for internet of things," *IEEE Internet Things J.*, vol. 5, no. 4, pp. 2605–2619, Aug. 2018.

[34] J. Tang, D. So, A. Shojaeifard, K. Wong, and J. Wen, "Joint antenna selection and spatial switching for energy efficient MIMO SWIPT system," *IEEE Trans. Wireless Commun.*, vol. 16, no. 7, pp. 4754–4769, Jul. 2017.

[35] W. Lu, Y. Gong, X. Liu, J. Wu, and H. Peng, "Collaborative energy and information transfer in green wireless sensor networks for smart cities," *IEEE Trans. Ind. Informat.*, vol. 14, no. 4, pp. 1585–1593, Apr. 2018.

[36] D. W. K. Ng, E. S. Lo, and R. Schober, "Energy-efficient resource allocation for secure OFDMA systems," *IEEE Trans. Veh. Technol.*, vol. 61, no. 6, pp. 2572–2585, Jul. 2012.

[37] Q. Wu, W. Chen, M. Tao, J. Li, H. Tang, and J. Wu, "Resource allocation for joint transmitter and receiver energy efficiency maximization in downlink OFDMA systems," *IEEE Trans. Commun.*, vol. 63, no. 2, pp. 416–430, Jun. 2018.


**Weidang Lu** (Senior Member, IEEE) received the Ph.D. degree in information and communication engineering from Harbin Institute of Technology, Harbin, China, in 2012.

He was a Visiting Scholar with the Nanyang Technology University, Singapore, The Chinese University of Hong Kong, Hong kong, and Southern University of Science and Technology, Shenzhen, China. He is currently an Associate Professor with the College of Information Engineering, Zhejiang University of Technology, Hangzhou, China. His current research interests include simultaneous wireless information and power transfer, wireless sensor networks, cooperative communications, and physical layer security for wireless systems.

**Xiaohan Xu** is currently working toward the master's degree in information and communication engineering with the Zhejiang University of Technology, Hangzhou, China.

Her current research interests include simultaneous wireless information and power transfer, wireless sensor networks, and cooperative communications.

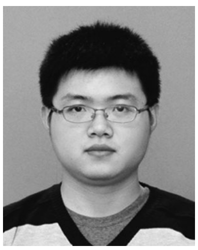

**Guoxing Huang** received the B.S. degree in measurement control technology and instruments from the University of Science and Technology, Beijing, China, in 2010, the M.S. degree in measuring and testing technologies and instruments from Liaoning University, Shenyang, China, in 2013, the Ph.D. degree in information and communication engineering from the Harbin Institute of Technology (HIT), Harbin, China, in 2019.

Since 2019, he has been an Associate Professor with the College of Information Engineering, Zhejiang University of Technology, Hangzhou, China. He has published more than 20 journal and conference papers. His current research interests include information acquisition theory, sampling with finite rate of innovation, compressive sensing, and signal processing.

**Bo Li** received the bachelor's degree in communication engineering and the master's and Ph.D. degrees in information and communication engineering from the Harbin Institute of Technology, Harbin, China, in 2007, 2009, and 2013, respectively.

He was a Visiting Ph.D. Student with the School of EEE, Nanyang Technological University, Singapore, from 2012 to 2013. Since 2013, he has been with the School of Information Science and Engineering, Harbin Institute of Technology, Weihai, China, as an Associate Professor. His current research interests include physical layer network coding, mobile ad hoc networks, and adaptive modulation and coding.

**Yuan Wu** (Senior Member, IEEE) received the Ph.D. degree in electronic and computer engineering from the Hong Kong University of Science and Technology, Hong Kong, in 2010.

He is currently an Associate Professor with the State Key Laboratory of Internet of Things for Smart City, University of Macau, Macao, China, and also with the Department of Computer and Information Science, University of Macau. Prior to that, he was a Full Professor with the College of Information Engineering, Zhejiang University of Technology, Hangzhou, China. During 2016–2017, he was a Visiting Scholar with the Department of Electrical and Computer Engineering, University of Waterloo. His current research interests include resource management for wireless networks, green communications and computing, mobile edge computing, and smart grids.

Prof. Wu received the Best Paper Award from the IEEE International Conference on Communications in 2016, and the Best Paper Award from IEEE Technical Committee on Green Communications and Computing in 2017. He served as the Guest Editors of IEEE Communications Magazine, IEEE Network, IEEE Transactions on Industrial Informatics, and *IET Communications*. He is currently on the Editorial Boards of IEEE Internet of Things Journal and *China Communications*.

**Nan Zhao** (Senior Member, IEEE) received the Ph.D. degree in information and communication engineering in 2011, from Harbin Institute of Technology, Harbin, China.

He is currently a Professor with Dalian University of Technology, Dalian, China.

Dr. Zhao is serving on the editorial boards of IEEE Wireless Communications, IEEE Wireless Communications Letters, and IEEE Transactions on Green Communications and Networking. He won the best paper awards in IEEE VTC 2017 Spring, ICNC 2018, WCSP 2018, and WCSP 2019. He also received the IEEE Communications Society Asia Pacific Board Outstanding Young Researcher Award in 2018.

**F. Reahard Yu** (Fellow, IEEE) received the Ph.D. degree in electrical engineering from the University of British Columbia (UBC), Vancouver, BC, Canada, in 2003.

From 2002 to 2006, he was with Ericsson, Lund, Sweden, and a start-up in California, USA. He joined Carleton University in 2007, where he is currently a Professor. His research interests include connected/autonomous vehicles, security, artificial intelligence, distributed ledger technology, and wireless cyber–physical systems.

Dr. Yu received the IEEE TCGCC Best Journal Paper Award in 2019, Distinguished Service Awards in 2019 and 2016, Outstanding Leadership Award in 2013, Carleton Research Achievement Award in 2012, the Ontario Early Researcher Award (formerly Premiers Research Excellence Award) in 2011, the Excellent Contribution Award at IEEE/IFIP TrustCom 2010, the Leadership Opportunity Fund Award from Canada Foundation of Innovation in 2009, and the Best Paper Awards at IEEE ICNC 2018, VTC 2017 Spring, ICC 2014, Globecom 2012, IEEE/IFIP TrustCom 2009, and International Conference on Networking 2005. He serves on the editorial boards of several journals, including Co-Editor-in-Chief for *Ad Hoc and Sensor Wireless Networks*, Lead Series Editor for IEEE Transactions on Vehicular Technology, IEEE Communications Surveys and Tutorials, and IEEE Transactions on Green Communications and Networking. He has served as the Technical Program Committee (TPC) Co-Chair of numerous conferences. He is a registered Professional Engineer in the province of Ontario, Canada, an IET Fellow, and Engineering Institute of Canada Fellow. The Web of Science Group has identified him as a Highly Cited Researcher. He is an IEEE Distinguished Lecturer of both Vehicular Technology Society (VTS) and Communication Society. He is an Elected Member of the Board of Governors of the IEEE VTS.